Proceedings Paper:
Griego, D, Buff, V, Hayoz, E et al. (2 more authors) (2017) Sensing and Mining Urban Qualities in Smart Cities. In: 2017 IEEE 31st International Conference on Advanced Information Networking and Applications (AINA). 2017 IEEE 31st International Conference on Advanced Information Networking and Applications (AINA), 27-29 Mar 2017, Taipei, Taiwan. IEEE , pp. 1004-1011. ISBN 978-1-5090-6029-0

https://doi.org/10.1109/aina.2017.14

Sensing and Mining Urban Qualities in Smart Cities

Danielle Griego
Chair of Information Architecture
ETH Zurich
Zurich, Switzerland
Email: griegod@ethz.ch

Varin Buff, Eric Hayoz, Izabela Moise and Evangelos Pournaras
Professorship of Computational Social Science
ETH Zurich
Zurich, Switzerland
Email: {buffv,ehayoz,imoise,epournaras}@ethz.ch

***Abstract*—The emergence of the Internet of Things in Smart Cities questions how the future citizens will perceive their predominant living and working environments and what quality of living they can experience within it, for instance the level of everyday stress. However, perception and experienced stress levels are challenging metrics to measure and are even more challenging to correlate with an underlying causal-effectual relationship in such stimulus abundant environments. The Internet of Things, enabled by several pervasive and ubiquitous devices such as smart phones and smart sensors, can provide real-time contextual information that can be used by advanced data science methodologies to generate new insights about urban qualities in Smart Cities and how they can be improved. The goal of this study is to show the predominant factors, which influence perceptual qualities of inhabitants in a Smart City equipped with sensing capabilities by the Internet of Things. To serve this goal, a novel data collection process for Smart Cities is introduced that involves (i) environmental data, such noise, dust, illuminance, temperature, relative humidity, (ii) location/mobility data, such as GNSS and citizens density detected via WiFi, and (iii) perceptual social data collected by citizens' responses in smart phones. These fine-grained real-time data can provide invaluable insights about the spatial correlations of the sensor measurements as well as the spatial and citizens' similarity illustrated. The data analysis illustrated reveals significant links between stress level and environmental changes observed.**

I. Introduction

The technological transformation of urban environments to Smart Cities enabled by the introduction of the Internet of Things poses challenges beyond technological ones. What urban qualities become predominant in this transformation? How citizens perceive modern urban environments and how quality of life influences factors such as the individuals' stress level? This paper illustrates a novel experiment in a real-world urban field designed for a fine-grained real-time sensing and mining of urban qualities in Smart Cities equipped with the Internet of Things.

The experiment involves the data collection of a broad spectrum of environmental and biofeedback physical/virtual sensors, as well as measurements of citizens' perception about their urban environment. The experiment involves 37 participants in the area of Zurich, Switzerland, who traverse a city path. The participants are equipped with several sensory devices and a smart phone through which they can express their perception about the urban environment they experience, for instance, how interesting, quiet, spacious or secure it is. This experimental methodology comes in contrast to other related experiments performed that either rely entirely on smart phone sensors [1], [2] or sensors embedded in public space and vehicles [3], [4]. Several technical challenges such as the automated detection of greenery and the data localization in the urban environment are tackled. The analysis of the collected data shows the spatial correlation between all pairs of sensor measurements. It also shows the similarity of urban spaces and citizens' groups. The illustrated data analysis can provide new insights about future applications of Smart Cities such as collective stress regulation, more intelligent policies for security and urban development, traffic management adjusted to citizens' life activity and others.

The contributions of this paper are summarized as follows: (i) A novel data collection process in a real-world urban field that involves a large spectrum of physical and virtual sensors in a fine-grained real-time mobile data collection process. (ii) The applicability of data science techniques for improving the quality of Smart City data collected via the Internet of Things. (iii) The mapping of citizens' perception onto several measurable urban indicators. (iv) A deeper understanding of urban qualities by mining spatial correlations of sensor measurements, the similarity of urban spaces and the similarity of citizens' groups from sensor data.

This paper is organized as follows: Section II compares the work of this paper with earlier related work. Section III illustrates the experimental methodology in a real-world urban field including information about the virtual sensors involved and methods of data localization. Section IV evaluates the collected data and studies the spatial correlation of the different sensor measurements. It also illustrates a method to measure the spatial and citizens' similarity. Finally, Section V concludes this paper and outlines future work.

II. Related Work

The experiment conducted in this study is designed as a follow-up to previous urban morphology perception studies, which explored the dynamics between urban spatial configurations and experiential qualities of space by inhabitants. This is of particular interest for urban planners due to the long-term nature of urban development decisions for street networks and building layouts. It is therefore important to further understand what types of public space promote desirable experiences. This is explored in an earlier study [5], which evaluates the relationships between urban spatial configurations along a select street network and subjective impressions through survey responses. Another study [6] follows a similar methodology but also includes physiological response data from participants using biofeedback wristbands.

Urban morphology as it is referred to in urban planning, is commonly represented through space syntax centrality measures and isovist properties. Space syntax analysis characterizes global spatial features such as visual access and accessibility between locations [7]. While isovist analyses quantifies local spatial features experienced from a given vantage point in space [8]. The studies conducted by [5], [9], [10] indicate that spatial qualities based on isovist analysis are linked to subjective experiences. In particular, the subjective experiences from the survey responses are statistically grouped into three categories: appeal (APP), experience (EXP) and activity (ACT) in the study performed by [5].

These experiments gather insightful information about experiential qualities of urban neighborhoods, but have yet to find a direct correlation between certain spatial configurations and positive or negative subjective ratings. For example, the study by [5] indicates that negatively rated areas are predominantly located in high traffic zones, while positively rated areas occur in pedestrian friendly zones. However both lack of contextual information about external environmental conditions such as temperature, noise, cloud cover, and people density, to show whether these also influence the rated experiences. Therefore, this work uses sensor-based environmental data to further explain whether environmental stress indicators, such as loud noise or levels of pollution are also associated with urban perception.

The experiment conducted in this study was originally designed to test the following hypotheses: Participants have a higher likability for spacious environments compared to narrow configurations as shown through subjective appraisal questionnaires, and irrespective of external conditions as shown through environmental sensor data. The results show that order and context highly influence subjective experience, and that it is less dependent on spatial configuration. In particular, the narrowest configuration (pathpoint 7) has the highest subjective rating along the experimental path, but shows to be the most ordered in terms of urban morphology and quite as measured by the sensor data. However, the analysis conducted in this paper goes a step further to investigate the complex dynamics of the urban experience using all collected time-series, geolocated data coupled with the subjective impression survey ratings. Using data science techniques, the spatial correlation of sensor measurements, as well as the spatial and citizens' similarity are illustrated for all measurement pairs.

III. Sensing Urban Qualities in Smart Cities

A data collection process is introduced that involves 37 participating citizens during the period 6th to 29th of April 2016. Sensing of citizens and their environment is performed along a path in the urban neighborhood environment of Alt-Wiedikon in Zurich, Switzerland, shown in Figure 1a and 1b. The path is chosen based on the alternation between static and dynamic urban features, however, emphasis is given on having highly distinguishable number and quality of spatial configurations, which change between narrow and spacious. Four instances of this transition along the path are observed in Figure 2.

Data were collected from six devices: (i) a biofeedback wristband, (ii) a WiFi receiver, (iii) a gas/environment sensorboard, (iv) temperature, relative humidity, illuminance sensor,

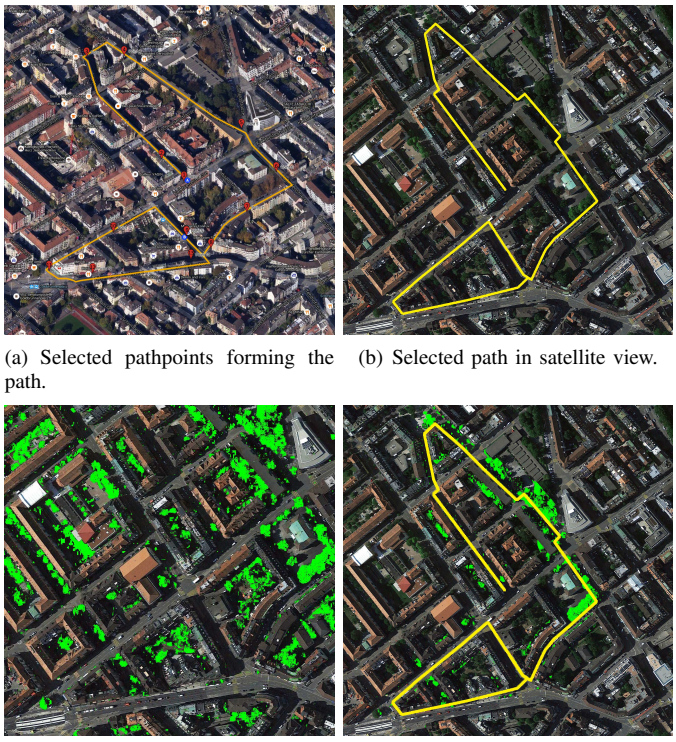

(a) Selected pathpoints forming the path.

(b) Selected path in satellite view.

(c) Greenery detection in the overall area.

(d) Greenery detection along the path.

Fig. 1. Pathpoints and greenery detection.

(v) GNSS device and (vi) a survey application on a smart phone. Each participant had to walk along the given path wearing the biofeedback wristband and carrying a "sensor-rucksack" equipped with mobile sensors. Each participant was accompanied by the same experiment moderator, who instructed them to respond to the mobile survey application at each of the 14 checkpoints along the path. This serves the purpose of removing the navigation duty from participants and shifts focus entirely on the designed experimental process. Completing the walk along the path required approximately 20-30 minutes depending on the casual walking pace of each participant.

At each of the 14 checkpoints along the path, the participants answer the mobile phone survey, shown in Figure 3, containing 12 qualitative questions to evaluate the environment they stand and experience. The purpose of the survey is to provide additional contextual labeling information to the sensor data collected and make the collected dataset more personalized. Table I illustrates the qualities rated on a five-point scale using survey questions appearing in mobile phones.

Table II illustrates the sensors from which measurements are recorded. The number of WiFi devices detected is used as an indicator of how populated is the environment and is referred to as people density (PD). The differential of the values collected from certain sensors is computed to measure change in values, rather than the actual values.

Table III illustrates the frequencies of data collection. A frequency reduction from 64 Hz and 4 Hz to 1 Hz is applied to the blood volume pressure (BVP) and electrodermal activity (EDA) respectively that are higher than the main frequency

TABLE I. QUESTIONS AND RANGES OF RATINGS FROM WHICH CITIZENS MAKE SELECTIONS. THE VIRTUAL SENSOR USING EACH QUESTIONS IS INDICATED.

Question #	1	2	3	4	5	6
Question Range	Beautiful Ugly	Empty - Crowded	Familiar - Unfamiliar	Interesting Boring	Light - Dark	Like - Dislike
Used in virtual sensor:	APP	-	APP	ACT	ACT	APP
Question #	7	8	9	10	11	12
Question Range	Open - Enclosed	Ordered Chaotic	Public Private	Quiet Noisy	Secure - Insecure	Spacious Narrow
Used in virtual sensor:	ACT	APP	APP	EXP	EXP	EXP

(a) Pathpoint 2, narrow (b) Pathpoint 3, spacious

(c) Pathpoint 4, narrow (d) Pathpoint 5, spacious

(e) Pathpoint 7, narrow (f) Pathpoint 8, spacious

(g) Pathpoint 10, narrow (h) Pathpoint 11, spacious

Fig. 2. Four instances of narrow-spacious spatial configurations and their corresponding pathpoints along the select path.

selection of 1 Hz. The average of 4 measurements is applied to the electrodermal activity (EDA) sensor since it is not an oscillatory value. The frequency of the blood volume pressure (BVP) is decreased by sampling the average of the 1st minute and subtracting this average from each raw value. At the final stage, the absolute values of the signal are derived. Figure 4 illustrates an example of the frequency reduction applied to a signal of blood volume pressure (BVP).

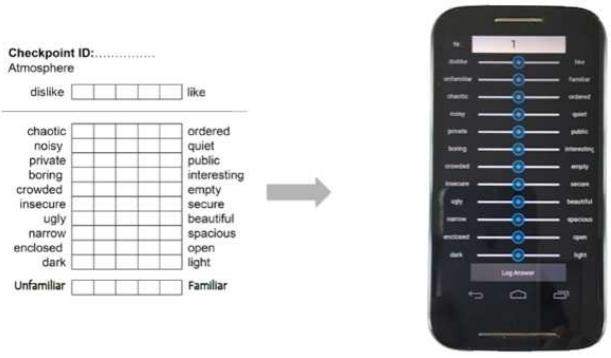

Fig. 3. The mobile app with the 12 criteria.

TABLE II. SENSORS FROM WHICH MEASUREMENTS ARE RECORDED. A SENSOR WITH A SECOND ACRONYM STARTING WITH '*d*' IS THE DIFFERENTIAL OF THE ORIGINAL ONE. THE SENSORS IN THE GREY BOXES ARE VIRTUAL SENSORS.

Acronym	Sensor description
PP	Path Point
HR, dHR	Heart Rate
BVP, dBVP	Blood Volume Pressure
EDA, dEDA	Electrodermal Activity
T-BF, dT-BF	Bio Feedback Temperature
S, dS	Sound
D, dD	Dust
T-EN, dT-EN	Environmental Temperature
RH, dRH	Relative Humidity
IL, dIL	Illuminance
ACC, dACC	Acceleration
PD	People Density
LON	Longitude
LAT	Latitude
GR	Greenery
APP	Appeal
ACT	Activity
EXP	Experience
SL	Stress Level

A. *Virtual sensors*

A *virtual sensor* is defined in this paper as non-physical sensor computed as a function of original measurements made from several physical sensors or survey answers. Three virtual sensors are discussed: (i) *greenery* (GR), (ii) *appeal* (APP), (iii) *activity* (ACT), (iv) *experience* (EXP) and (v) *stress* (SL).

Figure 1c illustrates the greenery (GR) detection performed over Google Earth satellite pictures around the area of the path. The greenery is detected by analyzing the RGB values of the pixels using the C++ library "CImg". Green pixels due to noise are excluded by checking cross neighbor pixels to classify the tested green pixels as true or false positive. The mapping of the GPS coordinates of the selected path to pixels is performed by converting WGS84 spherical coordinates of the GNSS receiver

TABLE III. DATA COLLECTION FREQUENCIES.

Sensor description	Frequency [Hz]
Heart rate (HR)	1
Blood volume pressure (BVP)	64
Electrodermal activity (EDA)	4
Biofeedback temperature (T-BF)	1
Sound level (S)	0.3
Dust (D)	0.3
Environment temperature (T-EN)	1
Relative humidity (RH)	1
Illuminance (IL)	1
People density (PD)	1 (if many), 0.024 (if few)
Longitude (LON)	1
Latitude (LAT)	1
Survey answers	In each of the 14 checkpoints

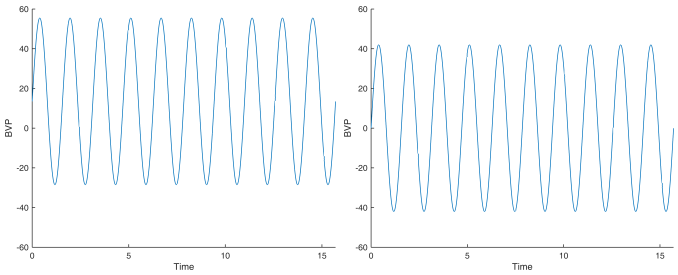

(a) Raw signal. (b) Signal after adding average offset.

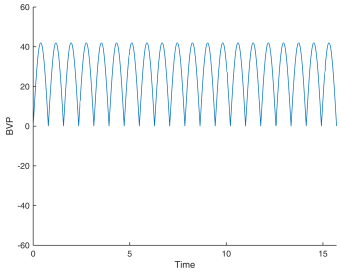

(c) Absolute positive signal.

Fig. 4. Frequency reduction applied to the bloom volume pressure measurements.

to the CH1903 planar coordinates and rescaling to the local pixel coordinates of the satellite pictures [11]. Measurements of greenery along the path are performed by recording the percentage of green pixels detected within a circle of 25 meters radius across each point of the path. Figure 1d shows the greenery detection along the path.

The virtual sensors of appeal (APP), activity (ACT) and experience (EXP) are formed from a subset of the survey questions as indicated in Table I. They specify features for the quality of the perceived urban environment. The three virtual sensors are documented in earlier work [5]. Each virtual sensor v_j provides a measurement at path point j given as follows:

$$v_j = \sum_{i=1}^{k} \frac{w_i(q_{i,j}+2)}{k}, \tag{1}$$

where k is the number of questions, $q_{i,j} \in [-2,2]]$ is the answer of a citizen in question i at path point j and w_i is a factor that weights the answer of a certain question i. Within the scope of this project, all questions are equally weighted.

The virtual sensor of *stress* (SL) is formed by the physical sensors of the biofeedback wristband, except the blood volume pressure (BVP) that generates highly noisy data. It represents the influence of the urban environment on the physical body activities of the citizens. Measurements of stress are evaluated in relation to a baseline that involves three-minute biofeedback wristband readings to obtain the low stress level frequency of each participant before the beginning of the experiment. The stress level is computed as follows:

$$v_j = \sum_{i=1}^{l-1} \frac{w_i s_{i,j}}{l-1}, \tag{2}$$

where l is the number of biofeedback sensors, $s_{i,j}$ is the normalized value of the biofeedback sensor i at path point j and w_i is a factor that weights the normalized value of the sensor i. Within the scope of this project, all biofeedback sensor values are equally weighted.

B. Data localization

Given that citizens participated in the experiments at different time points, the sensor data are studied in the spatial domain, meaning the path, which is fixed for all citizens. The sensor readings are geolocated by the GNSS devices, which however introduce some significant inaccuracies and mismatches of the localization on the path. Corrections are made by introducing heuristic algorithms that traverse the path points and associate each path point with the geolocated sensor data that are at some shortest distance to this path point. Three algorithmic methods are tested: (i) *circular*, (ii) *elliptical* and (iii) *minimum distance*. Figure 5 illustrates the concept of each method.

The circular method defines a circle with certain radius around each point on the path. The average of the sensor data in the circle is determined as the sensor data of this pathpoint, unless no sensor data fall into the circle. In the latter case, the radius exponentially increases by 10% until sensor data are found. Algorithm 1 illustrates the circular method.

The elliptical method is similar to the circular method. Instead of a circle, an ellipse is used around each point in the path with $a = 3$ meters and $b = 12$ meters. The shortest axis of the ellipse points to the direction of the next point in the path, with the longest axis perpendicular to the shortest one. The size of the ellipse increases 10% as long as no geolocated sensor data are enclosed. Algorithm 2 illustrates the elliptical method.

The minimum distance method associates each geolocated sensor data to the point on the path at the shortest Euclidean distance. If several geolocated sensor data are associated with one pathpoint, the mean of the sensor data is computed. An artifact of this method is that it may leave points on the path without sensor data. Algorithm 3 illustrates the minimum distance method.

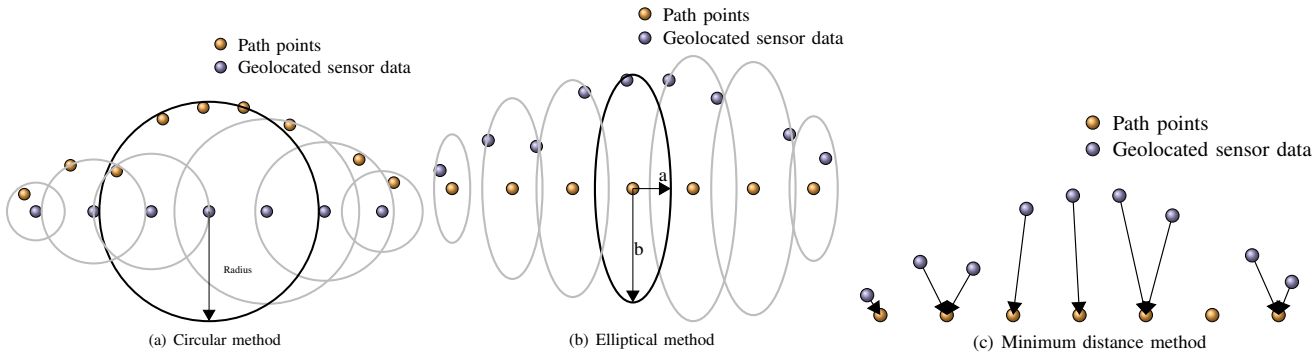

(a) Circular method (b) Elliptical method (c) Minimum distance method

Fig. 5. Three data localization methods.

Algorithm 1 The circle method for data localization

Require: path points, geolocated sensor data
for each consecutive path point **do**
  $r = 5m$, $c = 1$ and $i = 0$
  repeat
    for every geolocated sensor data **do**
      calculate distance d between path point and geolocated sensor data
      if $d \leq r \cdot c$ **then**
        add geolocated sensor data to path point
        $i++$
      end if
    end for
    if $i = 0$ **then**
      $c = c \cdot 1.1$
    end if
  until $i \neq 0$ or $c \geq 10$
  if $i \neq 0$ **then**
    get average of added geolocated sensor data
  end if
end for

Algorithm 2 The ellipse method for data localization

Require: path points, geolocated sensor data
for each consecutive path point except the last one **do**
  get $\vec{n}_1$ to next path point and the $\vec{n}_2$ perpendicular to $\vec{n}_1$
  $a = 3m$ for $\vec{n}_1$, $b = 12m$ for $\vec{n}_2$, $c = 1$ and $i = 0$
  repeat
    for every geolocated sensor data **do**
      calculate distances d_1 and d_2 between path point and geolocated sensor data in $\vec{n}_1$ and $\vec{n}_2$
      if $\frac{d_1^2}{c \cdot a^2} + \frac{d_2^2}{c \cdot b^2} \leq 1$ **then**
        add geolocated sensor data to path point
        $i++$
      end if
    end for
    if $i = 0$ **then**
      $c = c + 0.1$
    end if
  until $i \neq 0$ or $c \geq 10$
  if $i \neq 0$ **then**
    get average of added geolocated sensor data
  end if
end for

IV. Evaluation

The goal of the evaluation is to show how the sensor measurements can reveal the urban characteristics and perceptual experiences of the participating citizens traversing the urban path. Moreover, the evaluation aims at showing the spatial similarity as well as citizen group similarity using sensor measurements.

Algorithm 3 The lowest distance method for data localization

Require: path points, geolocated sensor data
for each geolocated sensor data **do**
  find path point with the lowest Euclidean distance
  add geolocated sensor data to path point
end for
for every path point **do**
  get average of added geolocated data
end for

The sensor values are normalized by dividing with the mean of all data points for each participating citizen. The python library scikit-learn[1] is used to implement the clustering algorithms for measuring the spatial and citizens similarity. The elliptical method is used for the data localization given that it provides higher accuracy than the cyclical method and associates geolocated sensor data to all pathpoints, in contrast to the minimum distance method. Moreover, the elliptical method can better tolerate signal reflections on walls that are usually perpendicular to the path for a citizen walking between buildings [12]. Exact quantitative results for the accuracy of each of the data localization methods are out of the scope of this paper.

A. Spatial sensing and mining

Figure 6 illustrates the sensor values among the checkpoints of the path. For each checkpoint, all sensor values of the citizens from the previous to the next checkpoint are averaged out. The biofeedback sensor values are shown in Figure 6a. The biofeedback temperature (T-BF) and heart rate (HR) remain at the same level over the path. However, the electrodermal activity significantly increases towards the last checkpoints of the path that indicate high moisture levels originated from sweating. The cause of this effect is subject of further investigation in future work and may be related to exposure in environmental noise, a biological function or the process of the experiment itself [13], [14], [15].

Figure 6b shows the environmental sensors. The sound (S) level is the highest at checkpoint 11 and 12 that are in crossroads of high traffic as can be seen in Figure 2. The dust (D) shows similar values with the sound. The environmental temperature (T-EN) does not vary significantly over the path.

[1] Available at http://scikit-learn.org/stable/ (last accessed: October 2016)

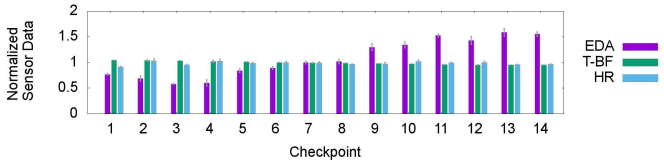

(a) Biofeedback sensors

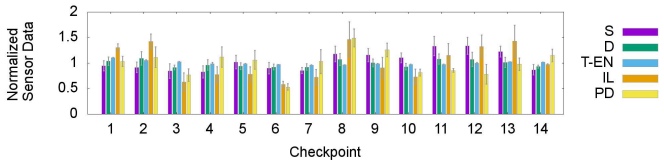

(b) Environmental sensors

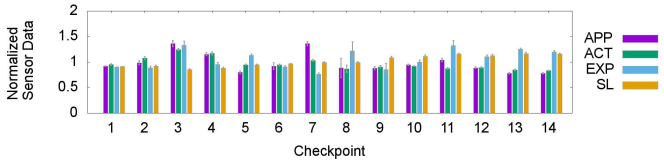

(c) Virtual sensors

Fig. 6. Normalized sensor values among checkpoints.

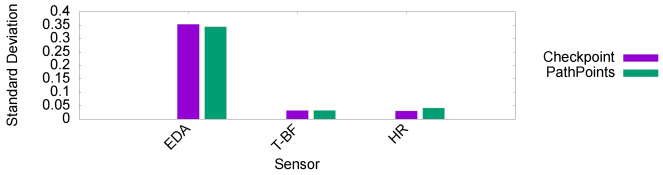

(a) Biofeedback sensors

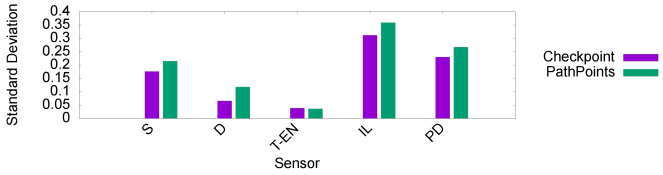

(b) Environmental sensors

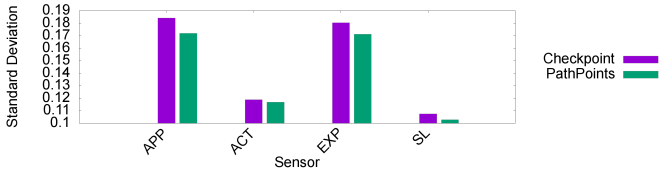

(c) Virtual sensors

Fig. 7. Standard deviation of the normalized sensor values over pathpoints and checkpoints.

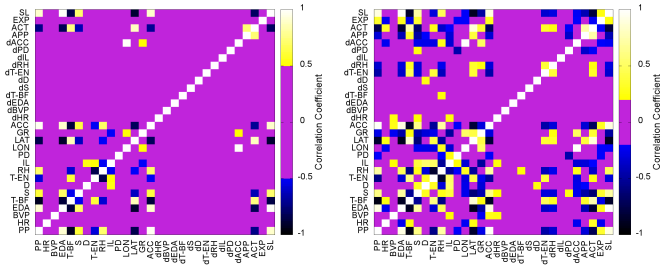

(a) Color mapping thresholds at ± 0.5. (b) Color mapping thresholds at ± 0.2.

Fig. 8. Correlation coefficient of all pair combination of the different data streams.

In checkpoints 1, 2, 8, 12, and 13, the illuminance (IL) is higher than in the other checkpoints. Finally, checkpoint 8 has the highest people density (PD).

Figure 6c shows the virtual sensors. Checkpoints 3, 4 and 7 have the highest appeal (APP) and activity (ACT). The park in checkpoint 3 may explain the high values in these checkpoints as shown in Figure 2. Checkpoints 3, 8 and 11 have the highest experience (EXP) values. The stress (SL) level is relatively stable, thus only a slight increase is observed as the path is traversed.

Figure 7 illustrates the standard deviation of the sensor values among the checkpoints and pathpoints after averaging out the sensor values over the citizens. Figure 7a shows the biofeedback sensors. The electrodermal activity (EDA) has the highest standard deviation as it significantly increases along the path. In the environmental sensors of Figure 7b, the illuminance (IL) and people density (PD) vary the most along the path. Among the virtual sensors of Figure 7c, the appeal (APP) and experience (EXP) show the highest deviation.

B. Correlation of sensor measurements

Figure 8 illustrates the correlation coefficient matrix of all pair combinations of data streams, averaged out over the participants. Figure 8a and Figure 8b show the same measurements, however, in different color mappings used as thresholds to depict and distinguish positive from negative correlations. In Figure 8a the thresholds are ± 0.5 and in Figure 8b ± 0.2. The correlation coefficient matrix shows which measurement pairs of sensors reflect correlated changes in the urban environment.

Figure 8b shows positive correlations in (i) acceleration (ACC) - electrodermal activity (EDA), (ii) acceleration (ACC) - sound (S), (iii) acceleration (ACC) - stress level (SL), (iv) stress level (SL) - electrodermal activity (EDA) and (v) appeal (APP) - activity (ACT). These results indicate that acceleration influences biofeedback measurements and citizens perceive an appealing urban environment as one with high activity, presumably because of the high values that green areas such as parks receive. Negative correlations are observed in (i) biofeedback temperature (T-BF) - acceleration, (ii) biofeedback temperature (T-BF) - stress level (SL), (iii) biofeedback temperature (T-BF) - electrodermal activity (EDA) and (iv) relative humidity (RH) - environmental temperature (T-EN). A plausible explanation of the first three negative correlations is an increased moisture levels from sweating, however, further evaluation through decomposition of all biofeedback data is part of future work. The negative correlation between relative humidity and environmental temperature is documented in earlier work [16] and it is expected for the temperate climate of Zurich.

C. Spatial and citizens similarity

Figure 9 illustrates the mean jaccard index between all pairs of clusters computed by all pair combinations of the different data streams. The jaccard index is computed by the intersection

of the clusters between a pair of data streams divided by their union and is used in this section as a measure of similarity [17]. Clusters are computed with DBSCAN [18] with the number of clusters estimated with the reduce and enlarge methods[2] in the range $[2, 9]$. The clusters either contain (i) the path points or (ii) the participating citizens. The jaccard index measures the *spatial similarity* in the former case and the *citizens' similarity* in the latter case, using the sensor data streams pairs as input.

Figure 9a and 9b show the spatial similarity computed by the pairs of data streams among pathpoints. By looking at the reduce method, high spatial similarities are observed in the following pairs of sensors: (i) heart rate (HR) - stress level (SL), (ii) appeal (APP) - experience (EXP) and (iii) heart rate (HR) - biofeedback temperature (T-BF). Figure 9c and 9d show the citizens' similarity computed by the pairs of data streams among citizens. By looking at the reduce method, high citizens' similarity is also observed in heart rate (HR)-stress level (SL) and between the differentials of the environmental temperature (dT-EN), relative humidity (dRH) and illuminance (dIL).

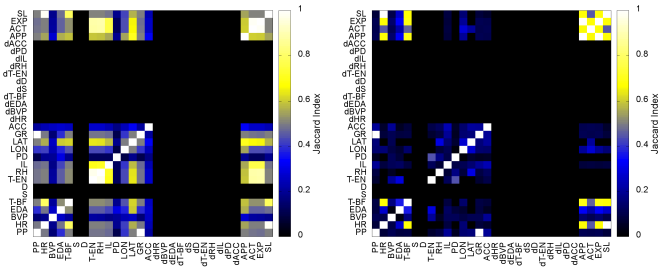

(a) 40 minimum samples/cluster, enlarge method, spatial similarity.

(b) 40 minimum samples/cluster, reduce method, spatial similarity.

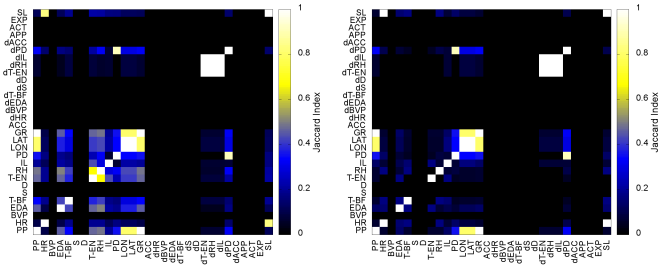

(c) 2 minimum samples/cluster, enlarge method, citizens' similarity.

(d) 2 minimum samples/cluster, reduce method, citizens' similarity.

Fig. 9. Mean jaccard index between all pairs of clusters computed by all pair combinations of the different data streams. Clusters are computed with DBSCAN with the number of clusters in the range $[2, 9]$. The spatial similarity is computed by the pairs of data streams among pathpoints and citizens' similarity among group of citizens.

Figure 10 illustrates the mean jaccard index between all pairs of clusters computed by all pair combinations of the different data streams. Clusters are computed with k-means. The number of clusters are detected by running the EM algorithm [19] by executing 100 iterations with 10 folds in cross-validation. The value of $1.0\text{E-}6$ is used for the minimum improvement in cross-validated log likelihood required to consider increasing the number of clusters and another iteration of the E and M steps as well as the minimum allowable standard deviation of normal density computation. Further validation with state-of-the-art validation indices [20] are out of the scope of this work given that this paper does not focus on k-means entirely. The spatial similarity is computed by the pairs of data streams among pathpoints. The citizens' similarity is omitted here due to its low number of data samples. Compared to DBSCAN in Figure 9, k-means shows increased similarity in the low similarity values of the DBSCAN, which is to be expected given that k-means is more sensitive to outliers and noise. However, DBSCAN shares the same high similarity pairs with k-means.

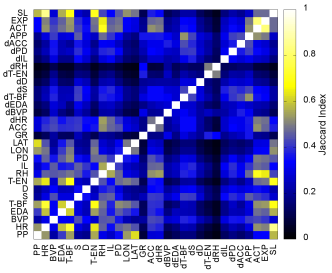

Fig. 10. Mean jaccard index between all pairs of clusters computed by all pair combinations of the different data streams. Clusters are computed with k-means with the number of clusters detected by running the EM algorithm. The context similarity is computed by the pairs of data streams among pathpoints.

V. Conclusion and Future Work

This paper concludes that sensing and mining data from urban environments equipped with the Internet of Things can provide new insights about urban qualities that can turn them into Smart City enablers. A broad spectrum of environmental information, biofeedback information and urban perceptual qualities can be measured in real-time via a novel data collection process in a real-world urban field that involves a broad spectrum of physical and virtual sensors. Data science methods are employed to understand spatial correlations of sensor measurements and the similarity of urban space and citizens' groups.

Future works includes the involvement of (i) a larger populations of citizens, (ii) annotated data about the patterns of users' activities (iii) decomposition analysis of electrodermal (EDA) data to determine phasic and tonic stress responses from participants (iv) building use-type, population density, and average income levels, (v) integration and comparison with other urban models, e.g. large-scale urban energy demand models and (vi) social interactions between the participating citizens to gain a deeper understanding of the dynamic urban qualities emerging in Smart Cities. A follow up of this study is the actual implementation and large-scale deployment of technology for sensing and mining several urban qualities using modular virtual sensors [21]. Emphasis will be given on privacy-preserving, participatory, ethical data collection and analytics methodologies [22], [23] supporting more sustainable and adaptive Smart Cities and digital societies [24].

[2]The reduce method incrementally decreases the ϵ value by 0.1 and evaluates the DBSCAN, resulting in minimum number of clusters possible within the given boundaries. The enlarge method follows the same process but increases the ϵ value resulting in maximum number of clusters possible within the given boundaries.

ACKNOWLEDGMENT

The experiment conducted in this study is funded by Swiss National Science Foundation project number 100013L_149552 under the DFG Research Grant for the project titled"ESUM-Analysing Trade-offs between the energy and social performance of urban morphologies". We would therefore like to acknowledge the direct and indirect contributions from the research staff, students and colleagues involved in the experimental set up. In particular Prof. Dr. Gerhard Schmitt, Dr Reinhard Konig, Matthias Standfest, Saskia Kuliga and Martin Bielik. A special thanks to Alesandro Forino for programming the mobile application and ensuring the proper functionality of the sensor backpack "sensor-rucksack". Last but not least, authors are thankful to the employees of Café Plüsch in Zurich for their hosting during the experiment and the 37 participants who participated in this study.

The data analysis presented in the paper is supported by the European Communitys H2020 Program under the scheme INFRAIA-1-2014-2015: Research Infrastructures, grant agreement #654024 SoBigData: Social Mining & Big Data Ecosystem (http://www.sobigdata.eu) and the European Communitys H2020 Program under the scheme ICT-10-2015 RIA, grant agreement #688364 ASSET: Instant Gratification for Collective Awareness and Sustainable Consumerism (http://www.asset-consumerism.eu).

REFERENCES

[1] N. Aharony, W. Pan, C. Ip, I. Khayal, and A. Pentland, "Social fmri: Investigating and shaping social mechanisms in the real world," *Pervasive and Mobile Computing*, vol. 7, no. 6, pp. 643–659, 2011.

[2] G. Cardone, L. Foschini, P. Bellavista, A. Corradi, C. Borcea, M. Talasila, and R. Curtmola, "Fostering participaction in smart cities: a geo-social crowdsensing platform," *IEEE Communications Magazine*, vol. 51, no. 6, pp. 112–119, 2013.

[3] S. Latre, P. Leroux, T. Coenen, B. Braem, P. Ballon, and P. Demeester, "City of things: An integrated and multi-technology testbed for iot smart city experiments," in *2016 IEEE International Smart Cities Conference (ISC2)*, Sept 2016, pp. 1–8.

[4] L. Sanchez, L. Muoz, J. A. Galache, P. Sotres, J. R. Santana, V. Gutierrez, R. Ramdhany, A. Gluhak, S. Krco, E. Theodoridis, and D. Pfisterer, "Smartsantander: Iot experimentation over a smart city testbed," *Computer Networks*, vol. 61, pp. 217 – 238, 2014.

[5] M. Bielik, S. Schneider, S. Kuliga, M. Valášek, and D. Donath, "Investigating the effect of urban form on the environmental appraisal of streetscapes."

[6] I. H. Hijazi, R. Koenig, S. Schneider, X. Li, M. Bielik, G. N. J. Schmit, and D. Donath, "Geostatistical analysis for the study of relationships between the emotional responses of urban walkers to urban spaces," *International Journal of E-Planning Research (IJEPR)*, vol. 5, no. 1, pp. 1–19, 2016.

[7] B. Hillier and J. Hanson, *The social logic of space*. Cambridge university press, 1989.

[8] M. L. Benedikt, "To take hold of space: isovists and isovist fields," *Environment and Planning B: Planning and design*, vol. 6, no. 1, pp. 47–65, 1979.

[9] S. Kuliga, R. C. Dalton, and C. Hölscher, "Aesthetic and emotional appraisal of the seattle public library and its relation to spatial configuration," in *Proceedings of the Ninth International Space Syntax Symposium (Seoul: Sejong University)*, 2013.

[10] G. Franz, M. Von Der Heyde, and H. H. Bülthoff, "An empirical approach to the experience of architectural space in virtual realityexploring relations between features and affective appraisals of rectangular indoor spaces," *Automation in Construction*, vol. 14, no. 2, pp. 165–172, 2005.

[11] W. Featherstone and P. Vanicek, "The role of coordinate systems, coordinates and heights in horizontal datum transformations," *Australian surveyor*, vol. 44, no. 2, pp. 143–150, 1999.

[12] J. Karedal, F. Tufvesson, T. Abbas, O. Klemp, A. Paier, L. Bernadó, and A. F. Molisch, "Radio channel measurements at street intersections for vehicle-to-vehicle safety applications," in *Vehicular Technology Conference (VTC 2010-Spring), 2010 IEEE 71st*. IEEE, 2010, pp. 1–5.

[13] M. Benedek and C. Kaernbach, "A continuous measure of phasic electrodermal activity," *Journal of neuroscience methods*, vol. 190, no. 1, pp. 80–91, 2010.

[14] J. J. Braithwaite, D. G. Watson, R. Jones, and M. Rowe, "A guide for analysing electrodermal activity (eda) & skin conductance responses (scrs) for psychological experiments," *Psychophysiology*, vol. 49, pp. 1017–1034, 2013.

[15] J. Ogorevc, G. Gerak, D. Novak, and J. Drnovek, "Metrological evaluation of skin conductance measurements," *Measurement*, vol. 46, no. 9, pp. 2993 – 3001, 2013.

[16] R. J. Ross, W. P. Elliott, D. J. Seidel, and A.-I. Participating, "Lower-tropospheric humidity-temperature relationships in radiosonde observations and atmospheric general circulation models," *Journal of Hydrometeorology*, vol. 3, no. 1, pp. 26–38, 2002.

[17] G. J. Torres, R. B. Basnet, A. H. Sung, S. Mukkamala, and B. M. Ribeiro, "A similarity measure for clustering and its applications," *Int. J. Electr. Comput. Syst. Eng.*, vol. 3, no. 3, pp. 164–170, 2009.

[18] M. Ester, H.-P. Kriegel, J. Sander, X. Xu *et al.*, "A density-based algorithm for discovering clusters in large spatial databases with noise." in *Kdd*, vol. 96, no. 34, 1996, pp. 226–231.

[19] G. Celeux and G. Govaert, "A classification em algorithm for clustering and two stochastic versions," *Computational statistics & Data analysis*, vol. 14, no. 3, pp. 315–332, 1992.

[20] E. Rendón, I. Abundez, A. Arizmendi, and E. Quiroz, "Internal versus external cluster validation indexes," *International Journal of computers and communications*, vol. 5, no. 1, pp. 27–34, 2011.

[21] E. Pournaras, I. Moise, and D. Helbing, "Privacy-preserving ubiquitous social mining via modular and compositional virtual sensors," in *2015 IEEE 29th International Conference on Advanced Information Networking and Applications*. IEEE, 2015, pp. 332–338.

[22] E. Pournaras, J. Nikolic, P. Velásquez, M. Trovati, N. Bessis, and D. Helbing, "Self-regulatory information sharing in participatory social sensing," *EPJ Data Science*, vol. 5, no. 1, p. 1, 2016.

[23] E. Pournaras, M. Warnier, and F. M. Brazier, "A generic and adaptive aggregation service for large-scale decentralized networks," *Complex Adaptive Systems Modeling*, vol. 1, no. 1, p. 1, 2013.

[24] D. Helbing and E. Pournaras, "Society: Build digital democracy," *Nature*, vol. 527, pp. 33–34, 2015.